THE JOURNAL OF PHYSICAL CHEMISTRY A

ARTICLE

pubs.acs.org/JPCA

TD-CI Simulation of the Electronic Optical Response of Molecules in Intense Fields II: Comparison of DFT Functionals and EOM-CCSD

Jason A. Sonk and H. Bernhard Schlegel*

Department of Chemistry, Wayne State University, Detroit, Michigan 48202, United States

ABSTRACT: Time-dependent configuration interaction (TD-CI) simulations can be used to simulate molecules in intense laser fields. TD-CI calculations use the excitation energies and transition dipoles calculated in the absence of a field. The EOM-CCSD method provides a good estimate of the field-free excited states but is rather expensive. Linear-response time-dependent density functional theory (TD-DFT) is an inexpensive alternative for computing the field-free excitation energies and transition dipoles needed for TD-CI simulations. Linear-response TD-DFT calculations were carried out with standard functionals (B3LYP, BH&HLYP, HSE2PBE (HSE03), BLYP, PBE, PW91, and TPSS) and long-range corrected functionals (LC-ωPBE, ωB97XD, CAM-B3LYP, LC-BLYP, LC-PBE, LC-PW91, and LC-TPSS). These calculations used the 6-31G(d,p) basis set augmented with three sets of diffuse sp functions on each heavy atom. Butadiene was employed as a test case, and 500 excited states were calculated with each functional. Standard functionals yield average excitation energies that are significantly lower than the EOM-CC, while long-range corrected functionals tend to produce average excitation energies slightly higher. Long-range corrected functionals also yield transition dipoles that are somewhat larger than EOM-CC on average. The TD-CI simulations were carried out with a three-cycle Gaussian pulse (ω = 0.06 au, 760 nm) with intensities up to 1.26×10^{14} W cm^{-2} directed along the vector connecting the end carbons. The nonlinear response as indicated by the residual populations of the excited states after the pulse is far too large with standard functionals, primarily because the excitation energies are too low. The LC-ωPBE, LC-PBE, LC-PW91, and LC-TPSS long-range corrected functionals produce responses comparable to EOM-CC.

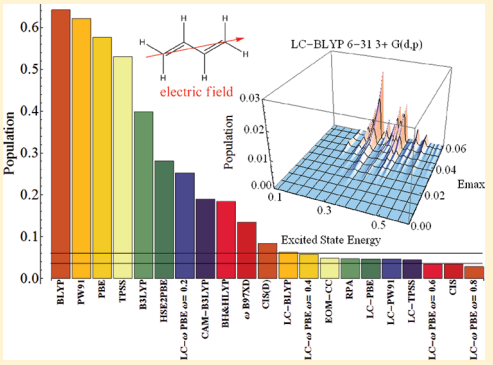

INTRODUCTION

A variety of strong field effects are observed when molecules are subjected to short, intense laser pulses (for recent progress, see refs 1−3). Because the electric fields of intense lasers are comparable to those sampled by valence electrons, the strong field response of a molecule cannot be treated by perturbative methods. Instead, numerical simulations are needed to model the nonlinear behavior of the electronic density interacting with intense electrical fields. Accurate grid-based simulation methods are available for few electron systems (for leading references, see refs 4 and 5). However, these methods cannot be used for larger polyatomic systems of interest in strong field chemistry. Two approximate methods that can be used for larger many-electron systems are (a) real-time integration of time-dependent Hartree−Fock (TD-HF) or density functional theory (TD-DFT), and (b) time-dependent configuration interaction (TD-CI). While the methodology for time-independent ground state electronic structure calculations has become well established, the techniques for reliable simulations of molecules in intense laser fields still need considerable testing. In a previous paper, we employed the TD-CI approach and compared the performance of various levels of wave function theory for calculating excited states, and tested the effects of basis set size and number of excited states used in the simulation. In the present paper we explore the utility of linear-response TD-DFT for calculating the field-free excitation energies and transition dipoles needed in TD-CI simulations. In a future paper, we will compare TD-CI simulations with real-time integration of TD-HF and TD-DFT.

Very simple molecules such as H_2^+ and H_2 have been studied extensively with accurate grid-based methods (see refs 4−5 and references therein). For larger many-electron systems, various approximate methods have been employed. TD-CI with grid based orbitals has been used for many electron atoms.[6] Some many-electron atoms and diatomics have been studied with TD-DFT with optimized effective potentials.[7−10] Cederbaum and collaborators[11−23] and Levine and co-workers[24−31] have used a multielectron dynamics to investigate hole migration following ionization. Klamroth, Saalfrank and co-workers[32−42] have employed time-dependent configuration interaction with single excitations (TD-CIS) to study electron dynamics, pulse shaping and ionization. Li and co-workers have used Ehrenfest dynamics and real-time integration of TD-DFT to investigate laser controlled dissociation processes.[43−45] In earlier studies we have used TD-HF and TD-CIS methods to simulate the response of

Received: July 7, 2011
Revised: September 15, 2011
Published: September 16, 2011

CO_2, polyenes, and polyacenes and their cations to short, intense laser pulses.[45−51]

The TD-CI approach for simulating the response of molecules to strong fields utilizes energies and transition dipoles for a large number of excited states calculated in the absence of a field. The least expensive methods for calculating these field-free excitation energies and transition dipoles are CIS, linear-response TD-HF (also known as the random phase approximation − RPA), and linear-response TD-DFT.[52,53] However, these methods do not include multielectron excitations. The effect of double excitations can be included in CIS calculations by perturbation theory with CIS(D)[54,55] or can be treated explicitly by configuration interaction calculations with singles and doubles (CISD). Multireference configuration interaction (MRCI) calculations can be used to include higher excitations. For systems too large for extensive MRCI calculations, the equation-of-motion coupled cluster method (EOM-CC)[56−59] is considered the method of choice for including electron correlation effects as well as higher excitations.

A good approximation to the time-dependent wave function is needed for calculating properties and observables. Ideally, one would like to compare various approximate methods for calculating the time-dependent wave function for a molecule in a laser field directly with experiment. However, the wave function is not an experimental observable, and the available observables are averages over many features of the wave function. Alternatively, one can compare approximate methods to a more accurate level of theory to identify promising approximations. Real-time integration of HF or DFT is known to have problems related to the representation of the wave function as a single Slater determinant of time-varying orbitals (for example, this leads to unphysical coupling between single and double excitation). In principle, TD-CI can reproduce the correct time dependence of the wave function, but in practice it is limited by the number, type, and accuracy of the time-independent states employed. In the present study, we choose to use the TD-CI approach and compare TD-CI simulations based on field-free excited states calculated with linear response TD-DFT with simulations based on more accurate excited states calculated by EOM-CCSD. These simulations are sufficient to point out very serious deficiencies in many of the functionals typically used to calculate excitation energies and to identify some promising functionals for strong field simulations.

In our previous paper,[51] we used the response of butadiene to short intense laser pulses (ω = 0.06 au, 760 nm with intensities up to 0.06 au, 1.26×10^{14} W cm^{-2}) as a test case. We compared the performance of TD-CI simulations with different numbers of excited states calculated using RPA, CIS, CIS(D), and EOM-CCSD with various basis sets. We found that the basis sets needed to include two or three sets of diffuse functions on each of the carbon atoms of butadiene, and that up to 500 excited states were needed for simulations for field strengths of 0.05 au. The EOM-CC calculations for so many states are rather expensive. The perturbative calculations in the CIS(D) method yield erratic results for the higher energy states. The CIS and TD-HF calculations are reliable but do not include the effects of electron correlation. Linear-response TD-DFT calculations do treat electron correlation, but there are many functionals to choose from. In the present paper, we again use butadiene in a short, intense laser pulse as a test case and examine TD-CI simulations with excitation energies and transition dipoles calculated by a representative set of density functionals.

METHODS

The time-dependent Schrödinger equation (TDSE) in atomic units is

$$i\frac{d\psi}{dt} = \hat{H}(t)\psi(t) \tag{1}$$

The time-dependent wave function, $\psi(t)$, can be expanded in terms of the ground state $|\varphi_0\rangle$ and excited states $|\varphi_i\rangle$ of the time-independent, field free Hamiltonian

$$\psi(t) = \sum_{i=0} C_i(t)|\varphi_i\rangle \tag{2}$$

Inserting eq 2 into eq 1 and multiplying from the left by $\langle\varphi_i|$ reduces the TDSE to a set of coupled differential equations for the time-dependent coefficients

$$i\frac{dC_i(t)}{dt} = \sum_j H_{ij}(t)C_j(t) \tag{3}$$

This expression can be integrated numerically using a unitary transform approach

$$\mathbf{C}(t + \Delta t) = \mathrm{e}^{-i\mathbf{H}(t+\frac{\Delta t}{2})\Delta t}\mathbf{C}(t) \tag{4}$$

In the dipole approximation, the matrix elements of the field-dependent Hamiltonian in eqs 3 and 4 can be expressed in terms of the field-free energies, ω_i, transition dipole moments, $\mathbf{D}_{ij}$, and the electric field, $\mathbf{e}(t)$.

$$\begin{aligned} H_{ij}(t) &= \langle\varphi_i|\hat{H}(t)|\varphi_j\rangle = \langle\varphi_i|\hat{H}_0|\varphi_j\rangle + \langle\varphi_i|\hat{r}|\varphi_j\rangle\cdot\mathbf{e}(t) \\ &= \omega_i\delta_{ij} + \mathbf{D}_{ij}\cdot\mathbf{e}(t) \end{aligned} \tag{5}$$

Analogous to the CIS treatment, the excited state to excited state transition dipoles for the density functional calculations are computed using the unrelaxed transition densities.

For the full solution of the TDSE, the sum in eq 3 extends over all bound states and the continuum. For practical applications, the sum needs to be restricted to a suitable subset of states. CIS, RPA, and TD-DFT calculations involve only single excitations. Errors in the valence excitation energies for CIS are typically 1 eV,[60] whereas TD-DFT methods can predict valence excitation energies within 0.5 eV.[52] The equation-of-motion coupled-cluster singles and doubles (EOM-CCSD) method treats electron correlation in the ground and excited states using the coupled-clusters approach. The EOM-CCSD method gives excitation energies that are within 0.3 eV of the experimental results for valence excited states.[60,61] To achieve even more accurate excitation energies, MRCI calculations would be needed, but the computational cost for larger molecules is prohibitive. A benefit of using TD-DFT is that excited state energies can be calculated at a fraction of the cost of EOM-CC and multireference methods. However, there are many different functionals and some may not be suitable for calculating the TD-CI simulations of molecules in strong fields.

The present study uses a linearly polarized and spatially homogeneous time-dependent external field,

$$\mathbf{e}(r,t) \approx \mathbf{E}(t)\sin(\omega t + \varphi) \tag{6}$$

This is a good approximation for the laser field, because typical wavelengths are much larger than molecular dimensions.

Table 1. Lowest Excitation Energies and Vertical IPs for Methods Used in This Study[a]

theoretical method	method type	first excited state energy in eV	calculated vertical IP in eV
	TD-DFT		
BLYP[87−89]	GGA	5.428	8.766
PBE[90,91]	GGA	5.428	8.940
PW91[90,92−95]	GGA	5.529	8.976
TPSS[96]	M-GGA	5.641	8.808
B3LYP[88,89,97]	H-GGA 20% HF	5.730	8.933
BH&HLYP[62,88,89,98]	H-GGA 50% HF	5.993	8.739
HSE2PBE (HSE03)[99,100]	H-GGA	5.641	9.157
LC-ωPBE[81,82,101,102]	LC	6.241	9.088
ωB97XD[77,103]	LC	5.998	8.951
CAM-B3LYP[104]	LC H-GGA 19−65% HF	5.962	8.987
LC-BLYP[87−89,105]	LC GGA	6.233	9.097
LC-PBE[90,91,105]	LC GGA	6.327	9.233
LC-PW91[90,92−95,105]	LC GGA	6.323	9.245
LC-TPSS[96,105]	LC M-GGA	6.334	9.195
	Wave Function-Based Methods		
UHF/CIS	SCF	6.415	7.697
ROHF/CIS	SCF	6.415	8.061
UCCSD	coupled-cluster	6.593	8.943
experiment		6.25[106]	9.072 ± 0.007[107]

[a] Calculated using the listed method and the 6-31 3+ G(d,p) basis set.

The simulations use a Gaussian envelope

$$g(t) = \exp[-\alpha(t/n\tau)^2] \quad (7)$$

$$\mathbf{E}(t) = \mathbf{E}_{max}[g(t - n\tau/2) - \Delta]/[1 - \Delta] \quad \text{for} \quad 0 \le t \ge n\tau$$
$$\mathbf{E}(t) = 0 \quad \text{for} \quad t < 0 \text{ and } t > n\tau$$

where $\tau = 2\pi/\omega$ is the period and n is the number of cycles. The offset Δ is chosen so that $\boldsymbol{E}(0) = 0$ and $\boldsymbol{E}(n\tau) = 0$. For $\omega = 0.06$ au (760 nm) and $\alpha = 16 \ln 2$, $\Delta = 1/16$, $n \approx 3$, and the full width at half-maximum (fwhm) ≈ 4 fs.

The DFT and EOM-CCSD calculations were carried out with the development version of the Gaussian software package.[62] The functionals used in this study are listed in Table 1 and were chosen to sample various aspects of DFT. TD-DFT can have substantial errors when charge-transfer excited states are involved. The use of long-range corrected functionals is one method of treating this error. Therefore, several long-range corrected functionals were considered (LC-ωPBE, ωB97XD, CAM-B3LYP, LC-BLYP, LC-PBE, LC-PW91, and LC-TPSS) in addition to a selection of standard functionals (B3LYP, BH&HLYP, HSE2PBE (HSE03), BLYP, PBE, PW91, and TPSS). To assess the effects of the range parameter in the long-range corrected functionals, calculations with LC-ωPBE were carried out with ω = 0.2, 0.4, 0.6, and 0.8. As in our previous studies,[51] *trans*-butadiene optimized at the HF/6-31G(d,p) level of theory was used as the test case. Excitation energies and transition dipoles were computed with the 6-31 3+ G(d,p) basis, which has one set of five Cartesian d functions on each carbon, one set of p functions on each hydrogen, and three sets of diffuse s and p functions on each carbon, with exponents of 0.04380, 0.01095, and 0.0027375. A three-cycle Gaussian pulse with ω = 0.06 au (760 nm) was used in the simulations. For maximal effect, the field was directed along the long axis of the molecule, specifically along the vector connecting the end carbons. As determined in our previous study,[51] up to 500 excited states were included in the simulations. Mathematica[63] was used to integrate the TD-CI equations and analyze the results. The TD-CI integrations were carried out with a step size of 0.5 au (0.012 fs). To achieve this step size, the time propagation in the TD-CI simulation utilized the exponential of the Hamiltonian matrix (see eq 4). The populations of the excited states after the pulse are shown in Figures 6 and 7 (to obtain smooth spectra, the excited state populations are plotted as Gaussians with an energy width of 0.01 au fwhm).

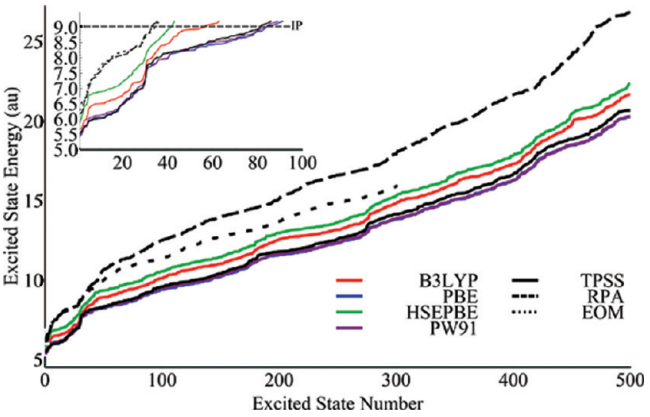

Figure 1. Excited state energies for the first 500 states of butadiene (all symmetries) calculated by standard density functionals: B3LYP (red), PBE (blue), HSEPBE (green), PW91 (purple) using the 6-31 3+ G(d,p) basis set. For comparison EOM-CC (black, dotted) and RPA (black, dashed) energies are included.

Table 2. Comparison of Average Excitation Energies, Average Transition Dipole Magnitudes, and the Sum of Excited State Populations[a]

theoretical method	average excitation energy in au	average transition dipole magnitude in au[b]	population of all excited states
	TD-DFT		
BLYP	0.3695	0.4590	0.6432
PBE	0.3760	0.4398	0.5796
PW91	0.3775	0.4466	0.5278
TPSS	0.3825	0.4393	0.5381
B3LYP	0.4038	0.4699	0.4101
HSE2PBE(HSE03)	0.4196	0.4620	0.2954
BH&HLYP	0.4441	0.5053	0.1977
LC-ωPBE $w = 0.2$	0.4140	0.5067	0.2631
LC-ωPBE $w = 0.4$	0.4680	0.5368	0.0705
LC-ωPBE $w = 0.6$	0.4962	0.5439	0.0436
LC-ωPBE $w = 0.8$	0.5100	0.5416	0.0359
ωB97XD	0.4399	0.5225	0.1441
CAM-B3LYP	0.4361	0.5176	0.2027
LC-BLYP	0.4743	0.5445	0.0749
LC-PBE	0.4809	0.5417	0.0561
LC-PW91	0.4816	0.5451	0.0576
LC-TPSS	0.4826	0.5382	0.0560
	Wave Function Based Methods		
EOM-CC	0.4540	0.4764	0.0640
RPA	0.4945	0.5281	0.0591
CIS	0.4950	0.5265	0.0454
CIS(D)	0.4432	0.5265	0.0986

[a] Calculated using 300 states and the 6-31 3+ G(d,p) basis set with a field strength of E_{max} = 0.05 au. [b] For transition dipoles with a magnitude greater than 0.001 au.

RESULTS AND DISCUSSION

Excitation Energies and Transition Dipoles. All of the methods agree that the lowest excited state of butadiene is ^1B_u and involves a single excitation from the highest occupied orbital to the lowest unoccupied orbital. Table 1 shows that the standard functionals underestimate the first excitation energy, while the long-range corrected functionals are in better agreement with experiment. For most of the functionals, the calculated ionization potential (IP) is within 0.2 eV of the experimental value (the exceptions are TPSS, BLYP and BH&HLYP). The standard functionals tend to be lower than the experimental IP and the long-range correct functionals are mostly higher. Thus, there is a qualitative agreement between the trends in the first excitation energy and the IP, but the relation is not quantitative ($R^2 = 0.42$).

Figures 1−4 compare the excited state energies for the functionals listed in Table 1. Table 2 lists the average excitation energies for first 300 excited states. The results seem to be grouped within the rungs of DFT's Jacob's ladder,[64] with the generalized gradient approximation (GGA) functionals (BLYP, PBE, and PW91) predicting the lowest average excitation energies. These are followed by TPSS, a metaGGA functional, while the highest average excitation energies correspond to hybrid functionals, B3LYP, HSE2PBE, and BH&HLYP. All of the standard functionals predict excited states that are on average

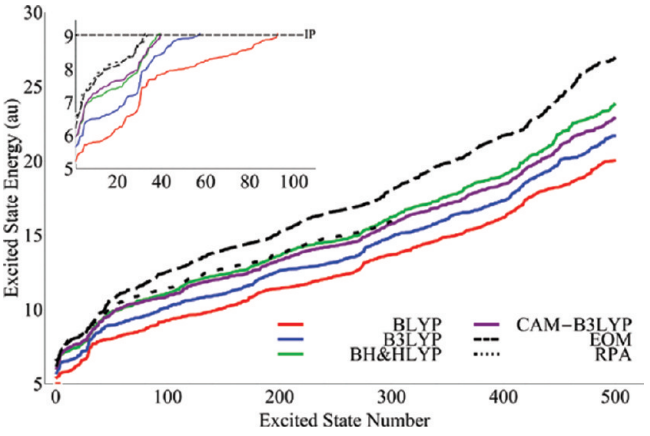

Figure 2. Effect of HF exchange for the first 500 excited states calculated using BLYP (0% HF, red), B3LYP (20% HF, blue), CAM-B3LYP (19−65% HF, purple), BH&HLYP (50% HF, green), EOM-CC (black, dotted), RPA (black, dashed). All methods used the 6-31 3+ G(d,p) basis set.

lower in energy than EOM-CC. Figure 1 shows the energies of the first 500 excited states of butadiene using some of the standard functionals listed in Table 1 (B3LYP, PBE, HSE2PBE, PW91, TPSS). Included in this figure are the excited state energies for the first 300 states calculated by EOM-CC and the first 500 states by RPA. Compared to the EOM-CC and RPA results, the TD-DFT excitation energies with the standard functionals are lower by as much as 4 eV for the highest energy states. The largest differences are for PBE, PW91, and TPSS. Compared to EOM-CC, the best performers among the standard functionals are BH&HLYP (−2%) and HSE2PBE (8%). The other standard functionals have differences in the average excitation energy greater than 10%. Mixing in a larger amount of HF exchange seems to reduce the error.

Figure 2 explores the effect of adding HF exchange to the BLYP functional: BLYP (no HF exchange), B3LYP (20% HF exchange), CAM-B3LYP (between 19 and 65% HF exchange), and BH&HLYP (50% HF exchange). As the amount of HF exchange increases from 0% to 50% the excited state energies approach those predicted by EOM-CC. The average error goes from −18% for BLYP to −11% B3LYP to −2% for BH&HLYP.

Most standard functionals have the wrong long-range behavior due to the self-interaction error.[65−69] As a result, the energies of Rydberg-like states are severely underestimated.[70−72] Increasing the amount of HF exchange in a global hybrid functional improves the long-range behavior, but degrades the performance at short-range. Long-range corrected functionals address this problem is by changing from an exchange functional at short-range to 100% HF exchange at long-range. This is achieved by using a switching function to divide the Coulomb operator into short-range and long-range parts.

$$\frac{1}{r_{12}} = \frac{\mathrm{erfc}(\omega r_{12})}{r_{12}} + \frac{\mathrm{erf}(\omega r_{12})}{r_{12}} \quad (8)$$

The parameter ω controls the ratio of these components as a function of distance. Figure 3 shows that excitation energies computed with long-range corrected functionals are in much better agreement with EOM-CC. The ωB97XD and CAM-B3LYP functionals predict energies ∼3−4% lower than EOM-CC, while the other long-range corrected functionals all predict

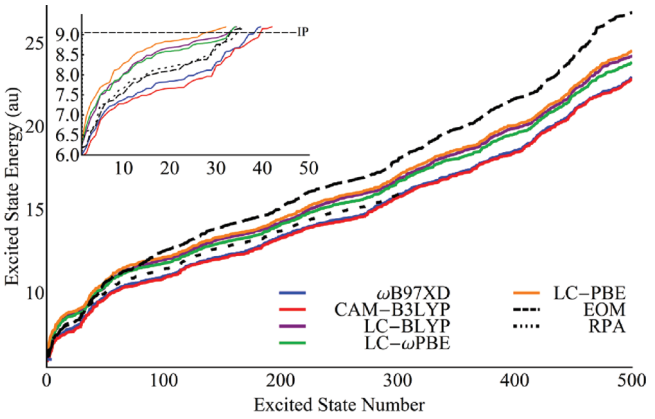

Figure 3. Excited state energies for the first 500 states of butadiene calculated by long-range corrected density functionals: ωB97XD (blue), CAM-B3LYP (red), LC-BLYP (purple), LC-ωPBE (green), LC-PBE (orange) using the 6-31 3+ G(d,p) basis set. For comparison EOM-CC (black, dotted), and RPA (black, dashed) energies are included.

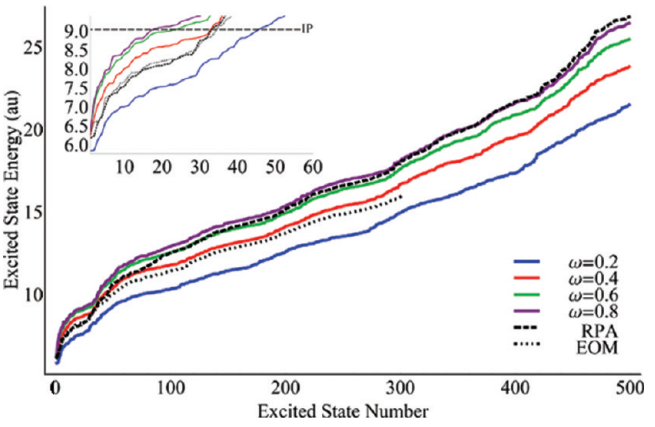

Figure 4. Excited state energies for the first 500 states of butadiene, calculated with LC-ωPBE/6-31 3+ G(d,p) and varying the ω-parameter: ω = 0.2 (blue), ω = 0.4 (default; red), ω = 0.6 (green), ω = 0.8 (purple); EOM-CC (black, dotted), and RPA (black, dashed) are included for comparison.

energies slightly higher than those of EOM-CC (LC-ωPBE 3%, LC-TPSS 6%, LC-PW91 6%, LC-PBE 6%, and LC-BLYP 4%).

Varying the ω-parameter changes the distance over which the switch from short-range to long-range behavior takes place. A relatively narrow range of ω values (from 0.2 to 0.5 bohr^{-1}) has been found by optimization of various properties for existing long-range corrected hybrid functionals.[73−86] Figure 4 demonstrates the effect on the excitation energies of changing the ω parameter in the LC-ωPBE functional. When ω is too small (more DFT exchange) the excitation energies are much lower than those of EOM-CC. If ω is too large (more HF exchange) the excitation energies are significantly higher than those of EOM-CC and approach the energies predicted by RPA/TD-HF (dashed line in Figure 4). A value of ω = 0.4 is best for reproducing the EOM-CC excited state energies. This is in agreement with the optimal value of ω = 0.4 found for calculating enthalpies of formation, barrier heights, and IPs.[81]

Correct transition dipoles should be just as important as accurate excitation energies for calculating the response to an intense laser field. A typical calculation yields several valence states below the IP with more Rydberg-like states growing closer together as the energy approaches the IP. A dense collection of states above the IP forms a pseudocontinuum. There are a few key valence states with large transition dipoles, which allow for efficient excitation from the ground state to excited states and from one excited state to another. In the pseudocontinuum, the transition dipoles are largest between neighboring states that have the highest spatial overlap and therefore the largest transition dipoles. A typical plot of the transition dipoles is shown in Figure 5 for the B3LYP functional. The magnitudes of the transition dipoles are plotted vertically; the ground state to excited state transition dipoles are along the horizontal axes and the excited-to-excited state transition dipoles make up the interior of the plot. The basis set dependence of the transition dipoles calculated with the B3LYP functional is similar to our previous study with CIS and RPA calculations.[51] The overwhelming majority of the transition dipoles are small in magnitude (of the more than 23 000 transition dipoles with magnitudes greater than 0.001 au, more than 15 000 have magnitudes less than 0.1 au), and only a relatively small number of transition dipoles have large magnitudes (less than 120 with magnitudes

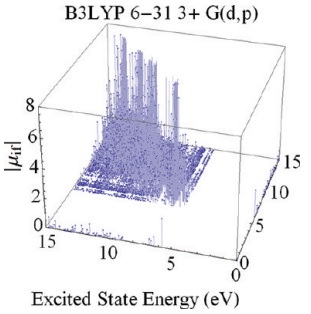

Figure 5. Transition dipoles for butadiene calculated with B3LYP/6-31 3+ G(d,p).

greater than 5 au). The statistical distributions of the transition dipoles are relatively similar across all of the density functional and wave function methods. The average magnitudes of the transition dipoles are compared in Table 2.

TD-CI Simulations of the Response to a Short, Intense Laser Pulse. The interaction of butadiene with a three-cycle Gaussian pulse (ω = 0.06 au, 760 nm; eq 6 and 7) was simulated with the TD-CI approach (eq 1−5) using excited states calculated with various density functionals. During the interaction with the laser field, many excited states contribute to the time-dependent wave function. Since the pulse is not resonant with any of the excitation energies, most of the populations of the excited states return to small values after the pulse. Because the interaction with the intense pulse is nonlinear, some population remains in the excited states after the field has returned to zero. These residual populations are a measure of the nonlinear response of the molecule interacting with the intense laser field and of the quality of the time-dependent wave function during and after the interaction with the laser pulse. If the nonlinear response (as measured by the residual populations) is too large or too small, then the approximate excitation energies and/or transition dipoles used in the TD-CI simulation are not suitable. Figures 6 and 7 show the residual populations of the excited states of butadiene after the pulse. The TD-CI simulations used 500 excited states, and the populations after the pulse are plotted

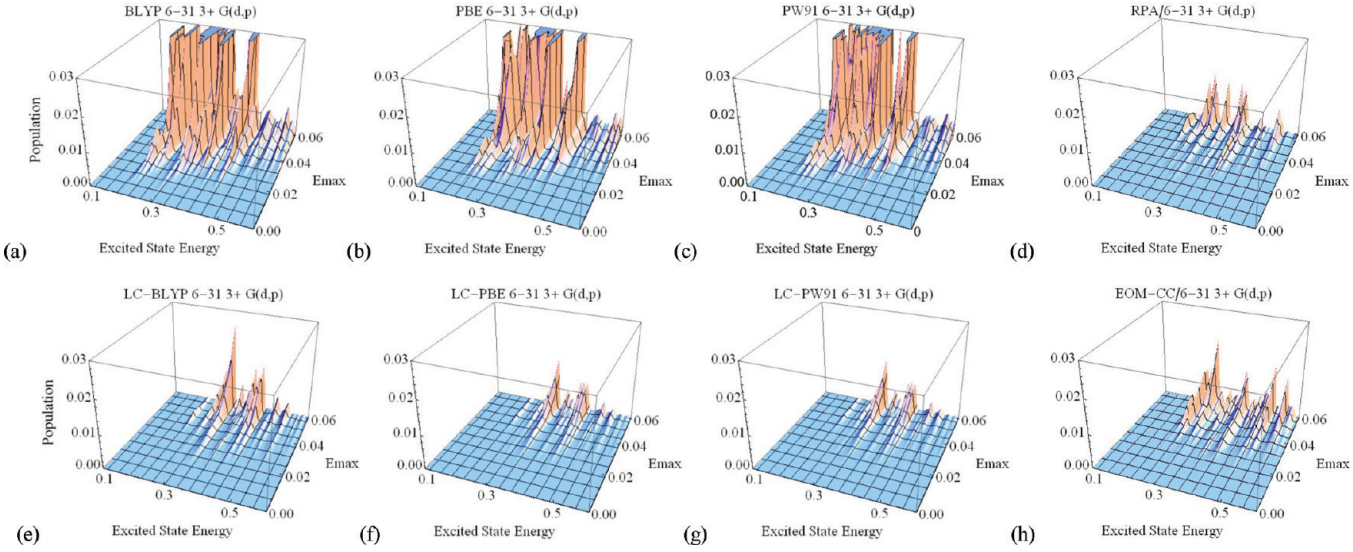

Figure 6. Excited state populations of butadiene after a three-cycle Gaussian pulse (ω = 0.06 au, E_{max} = 0−0.06 au) calculated with the 6-31 3+ G(d,p) basis set, using TD-CI with 500 states for the standard functionals (a) BLYP, (b) PBE, (c) PW91, and their long-range corrected counterparts (e)LC-BLYP, (f)LC-PBE, (g) LC-PW91, (d) RPA, and (h) EOM-CC (300 states).

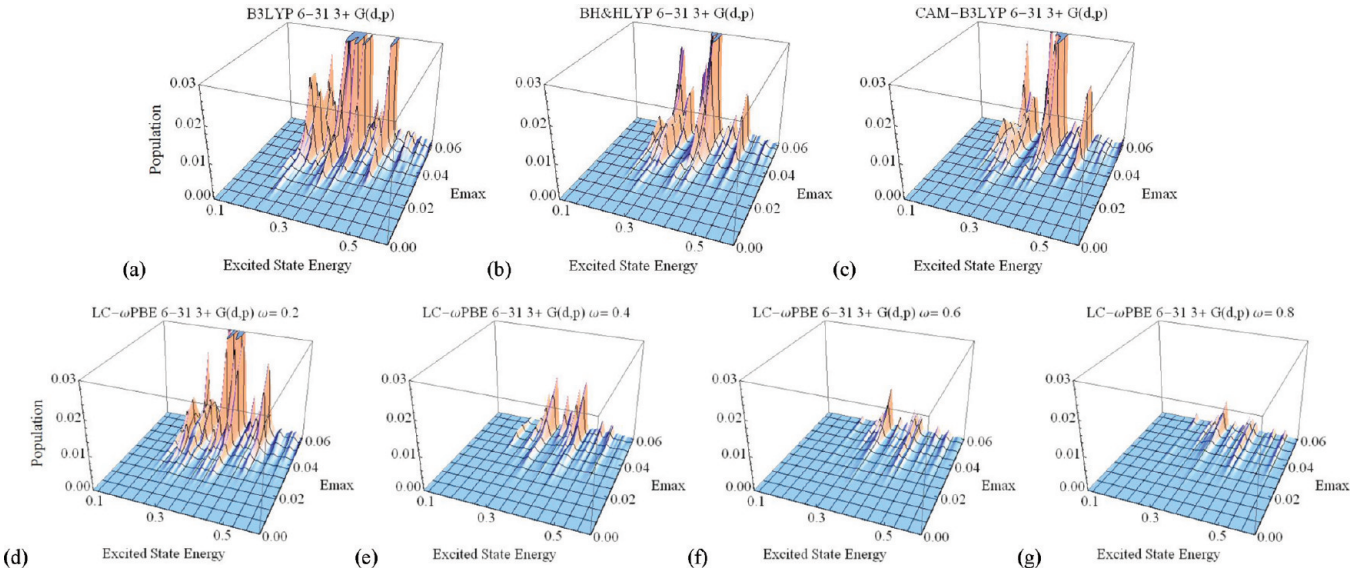

Figure 7. Excited state populations of butadiene after a three-cycle Gaussian pulse (ω = 0.06 au, E_{max} = 0−0.06 au) calculated with the 6-31 3+ G(d,p) basis set, using TD-CI with 500 states for (a) B3LYP, (b) BH&HLYP, (c) CAM-B3LYP, and LC-ωPBE with (d) ω = 0.2, (e) ω = 0.4 (default), (f) ω = 0.6, and (g) ω = 0.8.

as a function of the excited state energies and field strengths up to E_{max} = 0.06 au (1.26×10^{14} W/cm^2). As expected, the magnitude of the excitations increases rapidly with increasing field strength. Inspection of Figure 6 shows that the nonlinear response computed with BLYP, PBE, and PW91 is too strong compared to EOM-CC and RPA, while their long-range corrected counterparts are in much better agreement with EOM-CC and RPA. This indicates that long-range HF exchange is necessary. The effect of HF exchange is explored further in Figure 7. Figure 7a−c examines the effect of adding HF exchange to the BYLP functional. Mixing in HF character strongly affects the magnitude of the nonlinear response. B3LYP (20% HF exchange, Figure 7a) is much better than BLYP (0% HF exchange, Figure 6a). BH&HLYP (50% HF exchange, Figure 7b) and CAM-B3LYP (19− 65% HF exchange, Figure 7c) are a bit better than B3LYP, but the residual populations are still too large compared to EOM-CC (Figure 6h). This indicates that adding a percentage of HF exchange is not enough, and it is essential to switch to 100% HF exchange at long-range. The performance of long-range corrected DFT calculations can be sensitive to the choice of the range parameter. Figure 7d−g shows the effect of changing the ω in the LC-ωPBE functional. Too small of a value (switching to HF exchange at a longer range) yields residual populations that are too large compared to EOM-CC. Too large of a value of ω (switching to HF exchange at a shorter range) produces results that are much smaller than the EOM-CC.

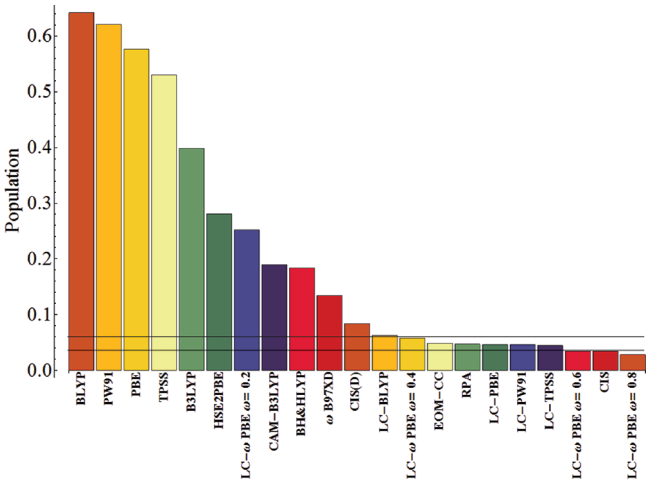

Figure 8. Comparison of the sum of the populations of the excited states with energies less than 0.5 au for TD-CI simulations based on DFT functionals and wave function calculations with the 6-31 3+ G(d,p) basis and 300 excited states. The horizontal lines represent the population of EOM-CC ± 25%.

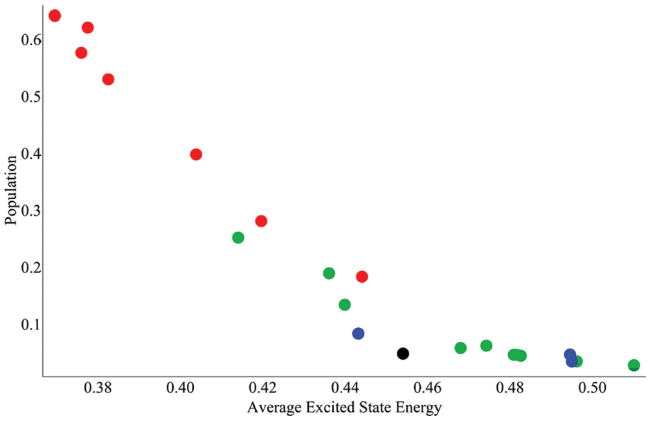

Figure 9. Correlation between the average excited state energy and the sum of the population of all excited states after the pulse calculated with the 6-31 3+ G(d,p) basis, E_{max} = 0.05 au and 300 states for the standard DFT functionals (red), long-range corrected functionals (green), wave function based methods (blue) and EOM-CC (black). (R^2 = 0.89 for a linear fit, and R^2 = 0.98 for a quadratic fit).

A more quantitative measure of the nonlinear response can be obtained by adding up the residual populations of the excited states generated by the pulse. Figure 8 and Table 2 compare the sum of the excited state populations for states with energies less than 0.05 au, based on simulations with E_{max} = 0.05 au and using 300 states. As noted previously,[51] RPA and CIS are in good agreement with EOM-CC, but the response of CIS(D) is a bit too strong. The nonlinear response for all of the standard functionals is far too strong. Most of the long-range corrected functionals fall within ±25% of the EOM-CC value. The exceptions are ωB97XD and CAM-B3LYP (too strong) and LC-ωPBE with ω = 0.8 (too weak).

Table 2 compares the sum of all excited states populations after the pulse for the various functionals, along with the average excitation energies and the average transition dipole magnitudes. The nonlinear response, as measured by the sum of the excited state populations after the pulse is not correlated with the calculated IP listed in Table 1 (R^2 = 0.01) and only weakly correlated with the average transition dipoles (linear fit R^2 = 0.14 for ground state to all excited states, R^2 = 0.58 for first excited states to all excited states, and R^2 = 0.42 for all transition dipoles; see Table 2). The nonlinear response is most strongly correlated with the first excitation energy (R^2 = 0.85) and the average excitation energy (Figure 9; R^2 = 0.89 for a linear fit, and R^2 = 0.98 for a quadratic fit). In particular, if the average excitation energy is significantly below the EOM-CC value, the response is far too strong. This is the case for most of the standard functionals. The average excitation energy for long-range corrected functionals is in better agreement with EOM-CC and the nonlinear response is comparable to EOM-CC.

CONCLUSIONS

The TD-CI approach has been used to examine the ability of various density functionals to simulate the interaction of butadiene with a short intense laser pulse. Excitation energies calculated by TD-DFT with standard functionals are significantly lower than the EOM-CC excitation energies. Long-range corrected functionals tend to produce average excitation energies slightly higher than EOM-CC. A value of ω = 0.4 in the LC-ωPBE functional provides good agreement with EOM-CC over a wide range of excitation energies. Long-range corrected functionals also yield transition dipoles that are larger than EOM-CC on average. The nonlinear response of butadiene interacting with an intense laser pulse is gauged by the residual populations of the excited states after the pulse. The nonlinear response computed by TD-CI simulations based on excitated states calculated with standard functionals is far too large, primarily because the excitation energies are too low. The response computed with long-range corrected functionals is comparable to that obtained with EOM-CC, RPA, and CIS. This indicates that correct long-range behavior is essential for the treatment of the diffuse and highly excited states needed to describe the interaction between the electron density and a strong laser field.

ACKNOWLEDGMENT

This work was supported by a grant from the National Science Foundation (CHE0910858). Wayne State University's computing grid and the NCSA Teragrid provided computational support. J.A.S. would like to thank the IMSD Program at WSU for financial support (GM058905-11).

REFERENCES

(1) *Strong Field Laser Physics*; Brabec, T., Ed.; Springer: New York, 2008.

(2) *Lectures on Ultrafast Intense Laser Science*; Yamanouchi, K., Ed.; Springer: New York, 2010.

(3) *Progress in Ultrafast Intense Laser Science I–VII*; Castleman, A. W., Jr., Toennies, J. P., Yamanouchi, K., Zinth, W., Series Eds.; Springer Series in Chemical Physics; Springer: Berlin/New York, 2006–2011.

(4) Schafer, K. J. Numerical methods in strong field physics. In *Strong Field Laser Physics*; Brabec, T., Ed.; Springer: New York, 2008; p 111.

(5) Kono, H.; Nakai, K.; Kanno, M.; Sato, Y.; Koseki, S.; Kato, T.; Fujimura, Y. Wavepacket dynamics of molecules in intense laser fields. In *Progress in Ultrafast Intense Laser Science IV*; Castleman, A. W., Jr., Toennies, J. P., Yamanouchi, K., Zinth, W., Series Eds.; Springer-Verlag: Berlin, 2008; pp 41.

(6) Greenman, L.; Ho, P. J.; Pabst, S.; Kamarchik, E.; Mazziotti, D. A.; Santra, R. *Phys. Rev. A* **2010**, *82*, 023406.
(7) Chu, S. I. *J. Chem. Phys.* **2005**, *123*, 62207.
(8) Heslar, J.; Telnov, D.; Chu, S. I. *Phys. Rev. A* **2011**, *83*, 043414.
(9) Telnov, D. A.; Chu, S. I. *Phys. Rev. A* **2009**, *79*, 041401.
(10) Telnov, D. A.; Chu, S. I. *Phys. Rev. A* **2009**, *80*, 043412.
(11) Breidbach, J.; Cederbaum, L. S. *J. Chem. Phys.* **2003**, *118*, 3983.
(12) Breidbach, J.; Cederbaum, L. S. *J. Chem. Phys.* **2007**, *126*, 034101.
(13) Hennig, H.; Breidbach, J.; Cederbaum, L. S. *J. Phys. Chem. A* **2005**, *109*, 409.
(14) Kuleff, A. I.; Breidbach, J.; Cederbaum, L. S. *J. Chem. Phys.* **2005**, *123*, 44111.
(15) Kuleff, A. I.; Cederbaum, L. S. *Chem. Phys.* **2007**, *338*, 320.
(16) Lünnemann, S.; Kuleff, A. I.; Cederbaum, L. S. *Chem. Phys. Lett.* **2008**, *450*, 232.
(17) Dutoi, A. D.; Cederbaum, L. S.; Wormit, M.; Starcke, J. H.; Dreuw, A. *J. Chem. Phys.* **2010**, *132*, 144302.
(18) Dutoi, A. D.; Wormit, M.; Cederbaum, L. S. *J. Chem. Phys.* **2011**, *134*, 024303.
(19) Kuleff, A. I.; Cederbaum, L. S. *Phys. Rev. Lett.* **2011**, *106*, 053001.
(20) Kuleff, A. I.; Lunnemann, S.; Cederbaum, L. S. *J. Phys. Chem. A* **2011**, *114*, 8676.
(21) Lünnemann, S.; Kuleff, A. I.; Cederbaum, L. S. *J. Chem. Phys.* **2008**, *129*, 104305.
(22) Lünnemann, S.; Kuleff, A. I.; Cederbaum, L. S. *J. Chem. Phys.* **2009**, *130*, 154305.
(23) Stoychev, S. D.; Kuleff, A. I.; Cederbaum, L. S. *J. Chem. Phys.* **2010**, *133*, 154307.
(24) Remacle, F.; Kienberger, R.; Krausz, F.; Levine, R. D. *Chem. Phys.* **2007**, *338*, 342.
(25) Remacle, F.; Levine, R. D. *J. Chem. Phys.* **1999**, *110*, 5089.
(26) Remacle, F.; Levine, R. D. *J. Chem. Phys.* **2006**, *125*, 133321.
(27) Remacle, F.; Levine, R. D. An electronic time scale in chemistry. *Proc. Natl. Acad. Sci. U.S.A.* **2006**, *103*, 6793.
(28) Remacle, F.; Levine, R. D. *Z. Phys. Chem.* **2009**, *221*, 647.
(29) Remacle, F.; Levine, R. D.; Ratner, M. A. *Chem. Phys. Lett.* **1998**, *285*, 25.
(30) Nest, M.; Remacle, F.; Levine, R. D. *New J. Phys.* **2008**, *10*, 025019.
(31) Periyasamy, G.; Levine, R. D.; Remacle, F. *Chem. Phys.* **2009**, *366*, 129.
(32) Klamroth, T. *J. Chem. Phys.* **2006**, *124*, 144310.
(33) Klinkusch, S.; Saalfrank, P.; Klamroth, T. *J. Chem. Phys.* **2009**, *131*, 114304.
(34) Krause, P.; Klamroth, T. *J. Chem. Phys.* **2008**, *128*, 234307.
(35) Krause, P.; Klamroth, T.; Saalfrank, P. *J. Chem. Phys.* **2005**, *123*, 74105.
(36) Krause, P.; Klamroth, T.; Saalfrank, P. *J. Chem. Phys.* **2007**, *127*, 034107.
(37) Nest, M.; Klamroth, T.; Saalfrank, P. *J. Chem. Phys.* **2005**, *122*, 124102.
(38) Tremblay, J. C.; Klamroth, T.; Saalfrank, P. *J. Chem. Phys.* **2008**, *129*, 084302.
(39) Tremblay, J. C.; Klinkusch, S.; Klamroth, T.; Saalfrank, P. *J. Chem. Phys.* **2011**, *134*, 044311.
(40) Tremblay, J. C.; Krause, P.; Klamroth, T.; Saalfrank, P. *Phys. Rev. A* **2010**, *81*, 063420.
(41) Huber, C.; Klamroth, T. *J. Chem. Phys.* **2011**, *134*, 054113.
(42) Klinkusch, S.; Klamroth, T.; Saalfrank, P. *Phys. Chem. Chem. Phys.* **2009**, *11*, 3875.
(43) Liang, W.; Isborn, C. M.; Lindsay, A.; Li, X. S.; Smith, S. M.; Levis, R. J. *J. Phys. Chem. A* **2010**, *114*, 6201.
(44) Liang, W. K.; Isborn, C. M.; Li, X. S. *J. Phys. Chem. A* **2009**, *113*, 3463.
(45) Li, X. S.; Smith, S. M.; Markevitch, A. N.; Romanov, D. A.; Levis, R. J.; Schlegel, H. B. *Phys. Chem. Chem. Phys.* **2005**, *7*, 233.
(46) Smith, S. M.; Li, X. S.; Markevitch, A. N.; Romanov, D. A.; Levis, R. J.; Schlegel, H. B. *J. Phys. Chem. A* **2005**, *109*, 5176.
(47) Smith, S. M.; Li, X. S.; Markevitch, A. N.; Romanov, D. A.; Levis, R. J.; Schlegel, H. B. *J. Phys. Chem. A* **2005**, *109*, 10527.
(48) Smith, S. M.; Li, X. S.; Markevitch, A. N.; Romanov, D. A.; Levis, R. J.; Schlegel, H. B. *J. Phys. Chem. A* **2007**, *111*, 6920.
(49) Smith, S. M.; Romanov, D. A.; Heck, G.; Schlegel, H. B.; Levis, R. J. *J. Phys. Chem. C* **2010**, *114*, 5645.
(50) Smith, S. M.; Romanov, D. A.; Li, X. S.; Sonk, J. A.; Schlegel, H. B.; Levis, R. J. *J. Phys. Chem. A* **2010**, *114*, 2576.
(51) Sonk, J. A.; Caricato, M.; Schlegel, H. B. *J. Phys. Chem. A* **2011**, *115*, 4678.
(52) Dreuw, A.; Head-Gordon, M. *Chem. Rev.* **2005**, *105*, 4009.
(53) Marques, M. A. L.; Gross, E. K. U. *Annu. Rev. Phys. Chem.* **2004**, *55*, 427.
(54) Headgordon, M.; Maurice, D.; Oumi, M. *Chem. Phys. Lett.* **1995**, *246*, 114.
(55) Headgordon, M.; Rico, R. J.; Oumi, M.; Lee, T. J. *Chem. Phys. Lett.* **1994**, *219*, 21.
(56) Kallay, M.; Gauss, J. *J. Chem. Phys.* **2004**, *121*, 9257.
(57) Koch, H.; Jorgensen, P. *J. Chem. Phys.* **1990**, *93*, 3333.
(58) Koch, H.; Kobayashi, R.; Demeras, A. S.; Jorgensen, P. *J. Chem. Phys.* **1994**, *100*, 4393.
(59) Stanton, J. F.; Bartlett, R. J. *J. Chem. Phys.* **1993**, *98*, 7029.
(60) Caricato, M.; Trucks, G. W.; Frisch, M. J.; Wiberg, K. B. *J. Chem. Theory Comput.* **2010**, *6*, 370.
(61) Schreiber, M.; Silva, M. R.; Sauer, S. P. A.; Thiel, W. *J. Chem. Phys.* **2008**, *128*, 134110.
(62) Frisch, M. J.; Trucks, G. W.; Schlegel, H. B.; Scuseria, G. E.; Robb, M. A.; Cheeseman, J. R.; Montgomery, J. A.; Vreven, T.; Kudin, K. N.; Burant, J. C.; Millam, J. M.; Iyengar, S.; Tomasi, J.; Barone, V.; Mennucci, B.; Cossi, M.; Scalmani, G.; Rega, N.; Petersson, G. A.; Nakatsuji, H.; Hada, M.; Ehara, M.; Toyota, K.; Fukuda, R.; Hasegawa, J.; Ishida, M.; Nakajima, T.; Honda, Y.; Kitao, O.; Nakai, H.; Klene, M.; Li, X.; Knox, J. E.; Hratchian, H. P.; Cross, J. B.; Bakken, V.; Adamo, C.; Jaramillo, J.; Gomperts, R.; Stratmann, R. E.; Yazyev, O.; Austin, A. J.; Cammi, R.; Pomelli, C.; Ochterski, J.; Ayala, P. Y.; Morokuma, K.; Voth, G. A.; Salvador, P.; Dannenberg, J. J.; Zakrzewski, V. G.; Dapprich, S.; Daniels, A. D.; Strain, M. C.; Farkas, Ö.; Malick, D. K.; Rabuck, A. D.; Raghavachari, K.; Foresman, J. B.; Ortiz, J. V.; Cui, Q.; Baboul, A. G.; Clifford, S.; Cioslowski, J.; Stefanov, B. B.; Liu, G.; Liashenko, A.; Piskorz, P.; Komaromi, I.; Martin, R. L.; Fox, D. J.; Keith, T.; Al-Laham, M. A.; Peng, C. Y.; Nanayakkara, A.; Challacombe, M.; Gill, P. M. W.; Johnson, B.; Chen, W.; Wong, M. W.; Gonzalez, C.; Pople, J. A. *Gaussian Development Version*; Revision H.10; Gaussian, Inc.: Wallingford, CT, 2010.
(63) *Mathematica*; 8.0 ed.; Wolfram Research, Inc.: Champaign, IL, 2010.
(64) Perdew, J. P.; Schmidt, K. *Density Functional Theory and Its Application to Materials*; Antwerp, Belgium, 8−10 June 2000; American Institute of Physics: Melville, NY, 2001.
(65) Dutoi, A. D.; Head-Gordon, M. *Chem. Phys. Lett.* **2006**, *422*, 230.
(66) Mori-Sanchez, P.; Cohen, A. J.; Yang, W. *J. Chem. Phys.* **2006**, *125*, 201102.
(67) Ruzsinszky, A.; Perdew, J. P.; Csonka, G. I.; Vydrov, O. A.; Scuseria, G. E. *J. Chem. Phys.* **2007**, *126*, 104102.
(68) Bally, T.; Sastry, G. N. *J. Phys. Chem. A* **1997**, *101*, 7923.
(69) Braida, B.; Hiberty, P. C.; Savin, A. *J. Phys. Chem. A* **1998**, *102*, 7872.
(70) Bauernschmitt, R.; Ahlrichs, R. *Chem. Phys. Lett.* **1996**, *256*, 454.
(71) Casida, M. E.; Jamorski, C.; Casida, K. C.; Salahub, D. R. *J. Chem. Phys.* **1998**, *108*, 4439.
(72) Tozer, D. J.; Handy, N. C. *J. Chem. Phys.* **1998**, *109*, 10180.
(73) Savin, A. *Recent Developments and Applications of Modern Density Functional Theory*; Elsevier: Amsterdam, 1996.
(74) Gerber, I. C.; Ángyán, J. G. *Chem. Phys. Lett.* **2005**, *415*, 100.

(75) Leininger, T.; Stoll, H.; Werner, H.-J.; Savin, A. *Chem. Phys. Lett.* **1997**, *275*, 151.
(76) Aron, J. C.; Paula, M.-S.; Weitao, Y. *J. Chem. Phys.* **2007**, *126*, 191109.
(77) Chai, J. D.; Head-Gordon, M. *J. Chem. Phys.* **2008**, *128*, 084106.
(78) Hisayoshi, I.; Takao, T.; Takeshi, Y.; Kimihiko, H. *J. Chem. Phys.* **2001**, *115*, 3540.
(79) Iann, C. G.; Janos, G. A.; Martijn, M.; Georg, K. *J. Chem. Phys.* **2007**, *127*, 054101.
(80) Jong-Won, S.; Tsuyoshi, H.; Takao, T.; Kimihiko, H. *J. Chem. Phys.* **2007**, *126*, 154105.
(81) Vydrov, O. A.; Heyd, J.; Krukau, A. V.; Scuseria, G. E. *J. Chem. Phys.* **2006**, *125*, 074106.
(82) Vydrov, O. A.; Scuseria, G. E. *J. Chem. Phys.* **2006**, *125*, 234109.
(83) Yoshihiro, T.; Takao, T.; Susumu, Y.; Takeshi, Y.; Kimihiko, H. *J. Chem. Phys.* **2004**, *120*, 8425.
(84) Jacquemin, D.; Wathelet, V.; Perpete, E. A.; Adamo, C. *J. Chem. Theory Comput* **2009**, *5*, 2420.
(85) Lange, A. W.; Rohrdanz, M. A.; Herbert, J. M. *J. Phys. Chem. B* **2008**, *112*, 6304.
(86) Ángyán, J. G.; Gerber, I. C.; Savin, A.; Toulouse, J. *Phys. Rev. A* **2005**, *72*, 012510.
(87) Becke, A. D. *Phys. Rev. A* **1988**, *38*, 3098.
(88) Lee, C. T.; Yang, W. T.; Parr, R. G. *Phys. Rev. B* **1988**, *37*, 785.
(89) Miehlich, B.; Savin, A.; Stoll, H.; Preuss, H. *Chem. Phys. Lett.* **1989**, *157*, 200.
(90) Perdew, J. P.; Burke, K.; Wang, Y. *Phys. Rev. B* **1996**, *54*, 16533.
(91) Perdew, J. P.; Burke, K.; Ernzerhof, M. *Phys. Rev. Lett.* **1997**, *78*, 1396.
(92) Burke, K.; Perdew, J. P.; Wang, Y. *Electronic Density Functional Theory: Recent Progress and New Directions*; Plenum Press: New York, 1998.
(93) Perdew, J. P. *Electronic Structure of Solids '91*: Proceedings of the 75th WE-Heraeus-Seminar and 21st Annual International Symposium on Electronic Structure of Solids held in Gaussig (Germany), ; Akademie Verlag: Berlin, 1991.
(94) Perdew, J. P.; Chevary, J. A.; Vosko, S. H.; Jackson, K. A.; Pederson, M. R.; Singh, D. J.; Fiolhais, C. *Phys. Rev. B* **1992**, *46*, 6671.
(95) Perdew, J. P.; Chevary, J. A.; Vosko, S. H.; Jackson, K. A.; Pederson, M. R.; Singh, D. J.; Fiolhais, C. *Phys. Rev. B* **1993**, *48*, 4978.
(96) Tao, J. M.; Perdew, J. P.; Staroverov, V. N.; Scuseria, G. E. *Phys. Rev. Lett.* **2003**, *91*, 146401.
(97) Becke, A. D. *J. Chem. Phys.* **1993**, *98*, 5648.
(98) Becke, A. D. *J. Chem. Phys.* **1993**, *98*, 1372.
(99) Heyd, J.; Scuseria, G. E.; Ernzerhof, M. *J. Chem. Phys.* **2006**, *124*, 219906.
(100) Paier, J.; Marsman, M.; Hummer, K.; Kresse, G.; Gerber, I. C.; Angyan, J. G. *J. Chem. Phys.* **2006**, *125*, 249901.
(101) Tawada, Y.; Tsuneda, T.; Yanagisawa, S.; Yanai, T.; Hirao, K. *J. Chem. Phys.* **2004**, *120*, 8425.
(102) Vydrov, O. A.; Scuseria, G. E.; Perdew, J. P. *J. Chem. Phys.* **2007**, *126*, 154109.
(103) Chai, J. D.; Head-Gordon, M. *Phys. Chem. Chem. Phys.* **2008**, *10*, 6615.
(104) Yanai, T.; Tew, D. P.; Handy, N. C. *Chem. Phys. Lett.* **2004**, *393*, 51.
(105) Iikura, H.; Tsuneda, T.; Yanai, T.; Hirao, K. *J. Chem. Phys.* **2001**, *115*, 3540.
(106) Saha, B.; Ehara, M.; Nakatsuji, H. *J. Chem. Phys.* **2006**, *125*, 014316.
(107) Lias, S. G. Ionization Energy Evaluation. In *NIST Chemistry WebBook*; NIST Standard Reference Database Number 69; National Institute of Standards and Technology: Gaithersburg, 2010.